

# Analysis and Suppression of Torsional Vibrations for the Permanent Magnet Synchronous Motor-Load System

Shiang Chih Fu, Stone Cheng  
Department of Mechanical Engineering, National Chiao-Tung University  
Hsinchu, Taiwan, ROC  
stonecheng@mail.nctu.edu.tw

**Abstract**—In motor transition system, different components, such as coupling, gears, and shaft are having different stiffness; they may be high or low. The low stiffness component will cause torsional vibration in the system, this phenomenon results in defect of products. In this paper, how the affection the parameters of a shaft caused to torsional vibration was discussed, and an adaptive notch filter is utilized to suppress the torsional oscillation, and then improve the bandwidth of the speed control loop. The adaptive notch filter can auto-identify the vibration frequency and auto-tune the parameters of the notch filter, achieving the objective of auto-suppressing torsional oscillation.

**Keywords**—PMSM, adaptive IIR notch filter, torsional vibration, suppress vibration, dual-inertia model, auto-tuning notch filter.

## I. INTRODUCTION

Generally, the driving methods in motor-load system can be separated into two types, one is the direct drive and another is coupled drive. The benefit in the direct drive is the system has a good dynamic characteristic, but when system re-designs or installs new mechanic devices, the cost and manufacture will be the main problem.

The advantage of the coupled drive way is its configuration and structure of the whole system are more flexible, and the prime cost is also lower, so the coupled drive is the common way in industry.

Gears, belts, couplings, and even shafts can be seen as linkage devices, driving the load part. The typical arrangement of mechanical system is shown in Fig. 1. In order to drive the load, the torque generated by motor transmits to shaft using reducer, if the stiffness of the shaft is not enough and the gears in reducer have backlash, the mechanical vibration will appear. This phenomenon can affect the system dynamic response, accuracy, and bandwidth, limiting the working efficiency.

For suppressing the torsional oscillation behavior and improving the bandwidth of the whole system, several ways and methods are suggested and raised. The simplest, convenient and direct methods are reducing the control gain on the speed loop, changing the speed command from step to ramp function, or increasing the stiffness of coupling devices [1]. The first and second methods affect the bandwidth of the

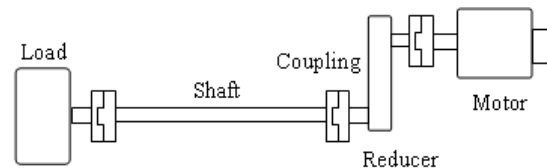


Figure 1. Typical arrangement of mechanical system.

speed loop, and then influence the transient response, the third has to face some matters such as parts manufacture, re-design and cost. So these methods are not the best choices.

The observer methods are the commonly used to improve the transient response of the dual-inertia system; repress the vibration behavior [2]-[6]. Although these methods can achieve better quality, the system would be sensitive for these state feedback values, and users have to understand the whole system, such as features of the structure, parameters of components, etc., for making a real-system-liked observer. The other inconvenience is that parameters are tuned at off-line state typically. Above disadvantages make observer difficult to be used in application.

The fifth method utilizes a notch filter to suppress the torsional vibration. This method has clarified its satisfactory effect in [7] and [8], but parameters of the notch filter also need to be modified manually. Various studies have been investigated in order to automatically detect the vibration frequency of a system and auto-tune the parameters of the notch filter for suppressing the mechanical vibration using adaptive notch filter, such as FFT method [9, 10], LMS/RLS method [11], and adaptive IIR notch filter method [12]. The main issue of these methods are the mass calculations at particular operation period [9, 10], difficult to realize [11], and only be applied in high frequency vibration (chattering phenomenon) repression [12].

This paper proposes a control structure based on the technique of adaptive IIR notch filter. Different from [12], the proposed method identified the frequency in real-time operation, and is applied to low frequency transient suppression, since most of the resonance frequencies for machinery are in the range of few tenths to few hundreds hertz.

In section III, the results show the good performance of the proposed control structure in the dual-inertia system with adaptive IIR notch filter.

## II. SYSTEM IDENTIFICATION

The block diagram of the proposed control system is shown in Fig. 2, where the transient vibration signal extractor derives the oscillation signal from the speed error, its function is similar to bandpass or highpass filter, and the output is sent to parameters adaptive tuning block for detecting the frequency of the error signal for modifying and estimating the parameters related to the notch filter. Finally, controller transmits these parameters into the notch filter to adjust the notch frequency.

The structure of the speed controller in Fig. 2 is based on the anti-windup, which is commonly used in feedback control application.  $K_p$ ,  $K_i$ , and  $K_a$  are proportional, integral and integral correction gain of the speed PI controller. The current control part consists of the PI controller and electric part in motor, its bandwidth is designed to 2000 Hz.

The following three sections (A~C) detail describes of dual-inertia system, geometric effect of a shaft and parameter adaptive tuning part.

### A. Dual-Inertia Model

In general application, loads are derived by shaft, and assumed in no damping situation. The dual-inertia system or said motor-load system can be simplified as Fig. 3(a) and its block diagram is shown in Fig. 3(b), where  $J_m$ ,  $J_L$ ,  $T_m$ ,  $T_L$ ,  $K_s$ ,  $\omega_m$  and  $\omega_L$  are the rotor inertia, load inertia, motor generate torque, disturbance torque, shaft stiffness, motor speed and load speed respectively.

Relationship between motor torque and motor speed is:

$$\frac{\omega_m}{T_m} = \frac{\frac{1}{J_m} \left( s^2 + \frac{1}{J_L} K_s \right)}{s^3 + \frac{(J_m + J_L)}{J_m \cdot J_L} K_s \cdot s} \quad (1)$$

From (1), we can get the resonance frequency and anti-resonance frequency shown in (2), (3).

$$\omega_{res} = \sqrt{K_s \cdot \frac{(J_m + J_L)}{J_m \cdot J_L}} \quad (rad/s) \quad (2)$$

$$\omega_{ares} = \sqrt{K_s \cdot \frac{1}{J_L}} \quad (rad/s) \quad (3)$$

Consequently, resonance and anti-resonance of the dual-inertia system are produced by motor and load side inertia and stiffness of the shaft. Notice that the resonance frequency is close to the anti-resonance frequency when load side inertia is very large compared with the motor side inertia.

### B. Geometric Effect of a Shaft

When the load inertia and rotor inertia both are fixed, from (2), the resonance frequency of the system will only be influenced by the stiffness of the shaft. For a shaft in cylinder shape, the stiffness is:

$$K_s = \frac{\pi r_o^4 G}{2L} \quad (N \cdot m / rad) \quad (4)$$

and for a hollow shaft:

$$K_s = \frac{\pi (r_o^4 - r_i^4) G}{2L} \quad (N \cdot m / rad) \quad (5)$$

where  $r_o$ ,  $r_i$ ,  $G$  and  $L$  are outside radius of the shaft, inside radius of the shaft, shear modulus and length of the shaft respectively.

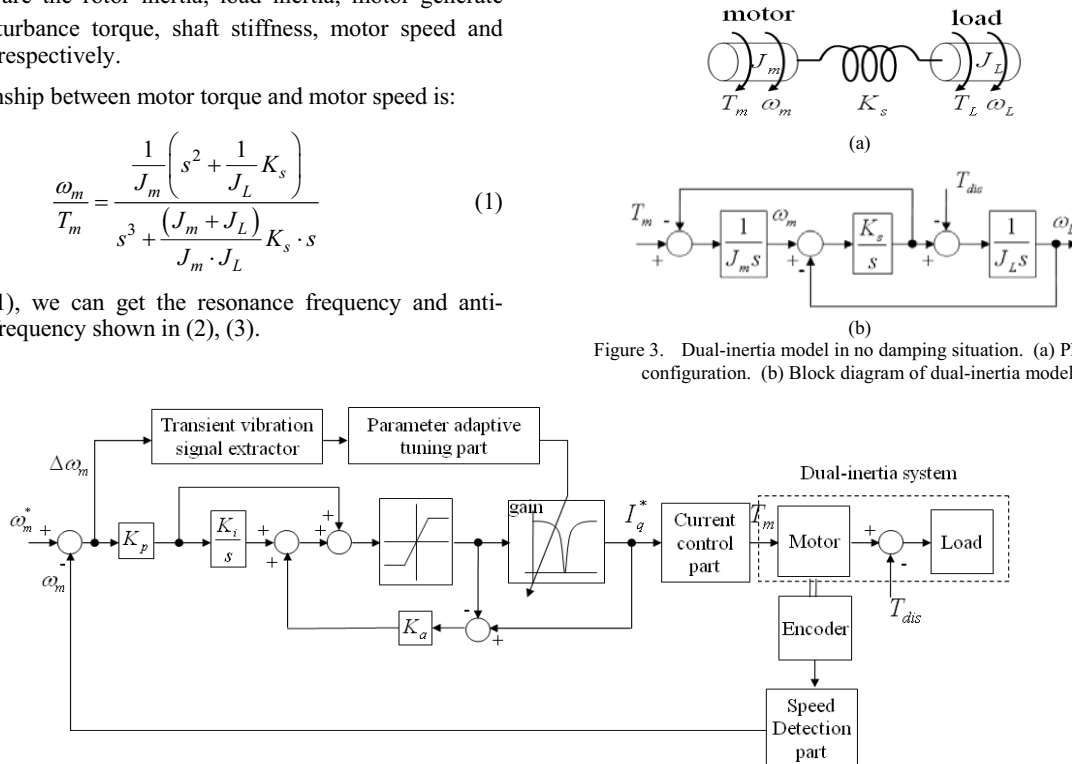
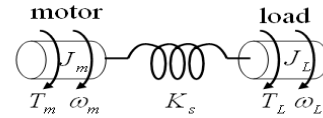
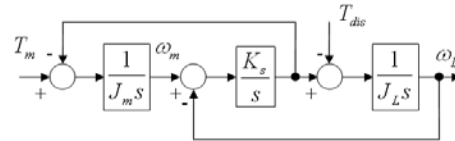


Figure 2. Proposed control system.



(a)



(b)

Figure 3. Dual-inertia model in no damping situation. (a) Physical configuration. (b) Block diagram of dual-inertia model.

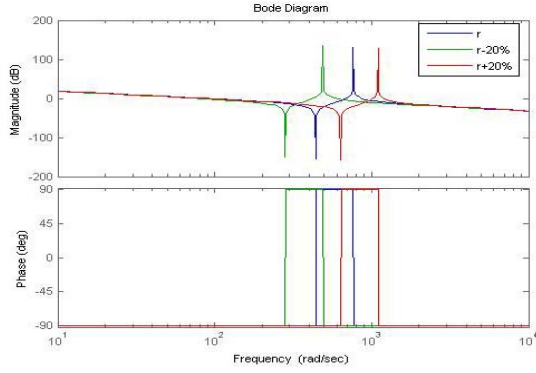


Figure 4. Frequency response of different outside radius of the shaft.

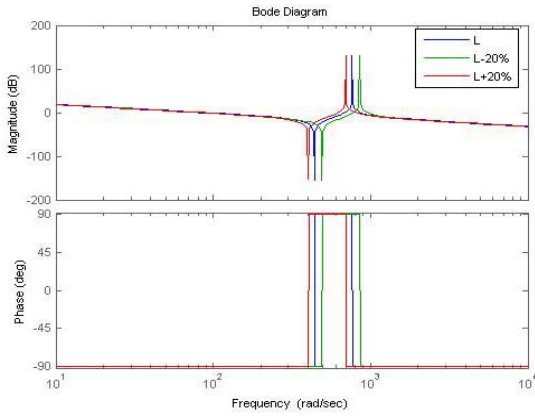


Figure 5. Frequency response of different length of the shaft.

For the same material, the shear modulus is identity, the radius of shafts affects the spring constant majorly, next is the length of the shaft, shown in (4) and (5) clearly.

Fig. 4 shows that different outside radius of the shaft changed the resonance frequency, and different lengths of the shaft altered the response shown in Fig. 5. Comparing these two figures, the frequency response variances for the different outside radius are greater than different lengths. It is an important knowledge for designing a shaft; the thicker and shorter the shaft is, the higher the resonance frequency is.

### C. Parameter Adaptive Tuning Part [13], [14], [15]

This part is an adaptive IIR notch filter, which is combined by four components: notch filter  $[H_N(z)]$ , bandpass filter  $[H_{BP}(z)]$ , partial sensitivity filter  $[H_P(z)]$ , and sensitivity filter  $[H_S(z)]$ , as shown in Fig. 6. Here, the bandpass filter is the ALE (adaptive line enhancement) structure, its function is enhancing the signal at certain desired frequency. Sensitivity filter and partial sensitivity filter are used to modify the parameters of the notch filter.

Equation (5) and (6) are the transfer function of the  $H_N(z)$  and  $H_S(z)$ .

$$H_N(z) = \frac{E(z)}{X(z)} = \left( \frac{2-a}{2} \right) \frac{1 - 2[(2-a-k^2)/(2-a)]z^{-1} + z^{-2}}{1 - (2-a-k^2)z^{-1} + (1-a)z^{-2}} \quad (5)$$

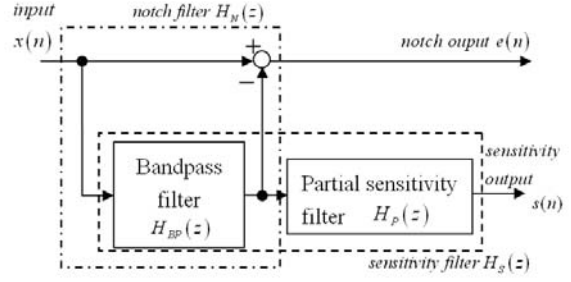


Figure 6. Parameter adaptive tuning part.

$$H_S(z) = \frac{S(z)}{X(z)} = \frac{a \cdot k (1+z^{-1})(1-z^{-1})z^{-1}}{[1 - (2-a-k^2)z^{-1} + (1-a)z^{-2}]^2} \quad (6)$$

where  $a$  determined the stop band, and  $k$  determined the notch frequency.  $a$  usually is a constant value to maintain a fixed stop band, only  $k$  is adjusted to let the notch frequency regulate to certain desired frequency.

Let  $a = 1 - r^2$  and  $k = \sqrt{1 + r^2 - 2r \cos \theta_p}$ , where  $r$  is the pole radius in the  $z$  domain,  $\theta_p$  is the normalized frequency, is defined as  $\theta_p = \omega_r / f_s$ , where  $\omega_r$  is the system vibration frequency (rad/sec),  $f_s$  is the sampling frequency (Hz), in this paper, the sampling frequency is 10 KHz. Then (5) can be simplified as (7):

$$H_N(z) = \frac{E(z)}{X(z)} = 1 - \frac{r^2 - 1}{2} \frac{(1+z^{-1})(1-z^{-1})}{1 - 2r \cos \theta_p z^{-1} + r^2 z^{-2}} \quad (7)$$

The adapting rules of the parameters  $k$  and  $p$  are shown in (8) and (9)

$$k(n+1) = k(n) - \mu \frac{e(n)s(n)}{p(n) + p_{\min}} \quad (8)$$

$$p(n+1) = \lambda p(n) + (1-\lambda) \|s(n)\|^2 \quad (9)$$

Where  $s(n)$  is the output of (6),  $p_{\min}$  is used to prevent the singularity.  $\mu$  is the positive quantity scaling factor or called step size parameter which affecting the rate of convergence and stability.  $\lambda$  is a forgetting factor, its value between zero and one.

### III. SYSTEM SET-UP AND RESULTS

In order to verify the proposed controller for two-inertia system, the rotating motion system is shown in Fig. 7. Fig. 8 is the simple representation for Fig. 7. The system is constructed by PMSM (Teco JSMA-MB10), couplings, shaft, flywheels, hysteresis brake and servo motor driver; corresponding parameters are listed in Table I.

Motor side inertia is formed by rotor and motor side flywheel, used to increase motor side inertia. Load side inertia is composed by hysteresis brake and load side flywheel; load

side flywheel can change the load side inertia as the motor side. Beside, hysteresis brake can be a disturbance generator.

The flexible shaft connects motor side and load side, the shaft can be treated as torsional spring, making the structure to have the characteristic of resonance vibration.

The following test cases are in the two different situations: for  $K_p=0.2$  and  $K_p=1$ . In this section, the parameters in tuning part is  $\mu = 0.008$ ,  $a = 0.0975$ ,  $P_{\min} = 0.001$ ,  $\lambda = 0.95$  and  $k(0) = 0.1$ ; and from the Table I, we can calculate some parameters such as shaft stiffness  $k$  and resonance frequency  $\omega_r$ , these value can be substituted into dual-inertia system shown in Fig. 2.

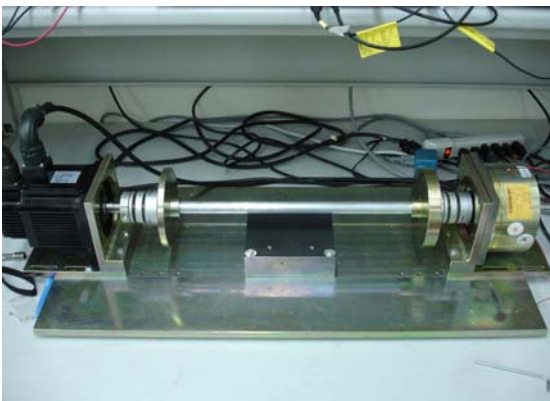


Figure 7. Experiment set up.

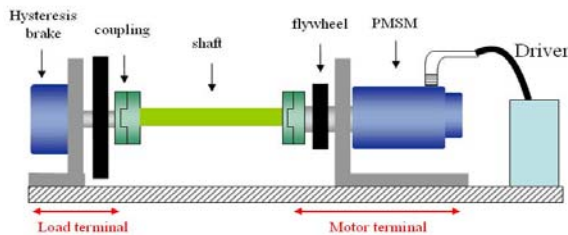


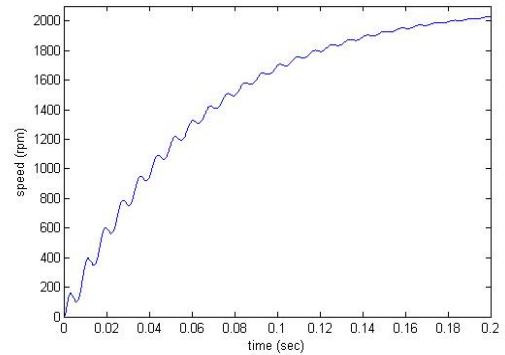
Figure 8. Simple representation of the set up.

A.  $K_p = 0.2$

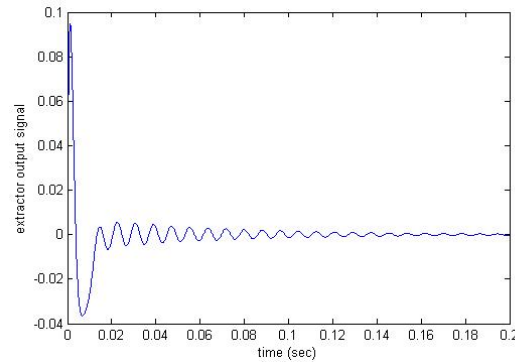
In this example, the motor speed response is shown in Fig. 9(a), which in the situation of no transient vibration signal extractor and no parameter adaptive tuning part.

It is clearly that the speed response vibrated during the raising period. In order to improve the transient response, suppress this phenomenon with no affection on the bandwidth, this paper uses transient vibration signal extractor and parameter adaptive tuning part to do the vibration control.

The oscillation signal shown in Fig. 9(b) is extracted from speed error signal by transient vibration signal extractor, and



(a)



(b)

Figure 9.  $K_p$  gain = 0.2 (a) Speed response. (b) Oscillation signal.

TABLE I. CHARACTERISTICS OF EACH ELEMENT

	shaft	Flywheel at motor side	Flywheel at load side	motor	Hysteresis brake
Inertia (kg-m <sup>2</sup> )	$1.9 \times 10^{-4}$	$3.073 \times 10^{-3}$	$6.145 \times 10^{-3}$	$6.37 \times 10^{-4}$	$1.45 \times 10^{-3}$
Outside radius (m)	$1.1 \times 10^{-2}$			$1.1 \times 10^{-2}$	$1.1 \times 10^{-2}$
Length (m)	~0.4	0.0106	0.0206		
Material	aluminum alloy	cast iron	cast iron		
Flywheel outside Radius (m)		0.07	0.7		
Flywheel inside Radius (m)		0.011	0.011		
Shaft stiffness (N-m/rad)	1500				
Resonance Frequency $\omega_r$ (rad/sec)	About 763.8rad/sec(121.56 Hz or 0.07638 normalized frequency)				

then it can obtain the normalized frequency of this vibration signal via the parameter adaptive tuning part, as shown in Fig. 10, where the initial value of normalized frequency is based on the initial value of  $k = 0.1$ ; this tuning part starts receiving the output of the signal extractor and calculating the algorithm at 0.01s.

The detected normalized frequency is about 0.0762 at 0.2s, which very closed to the exact value 0.07638. After this 0.2s time moment, parameters  $a$  and  $k$  are then sent into the notch filter, performing the vibration control.

In speed response shown in Fig. 11(a), during 0 to 1s, the vibration signals are sampled and the vibration frequency is

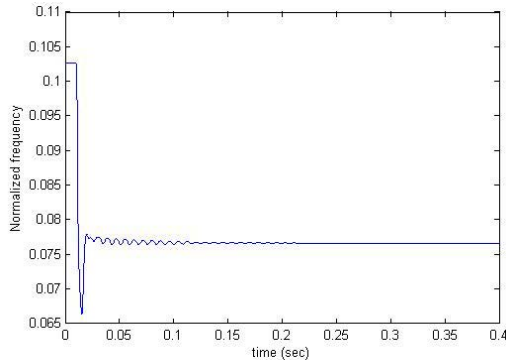
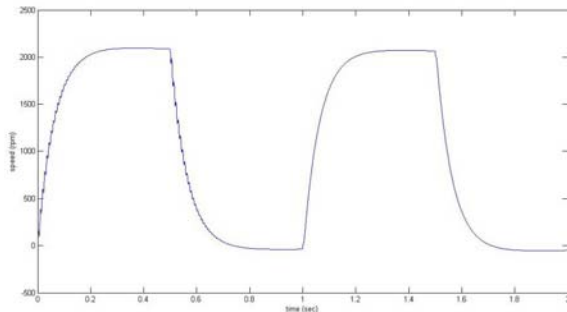
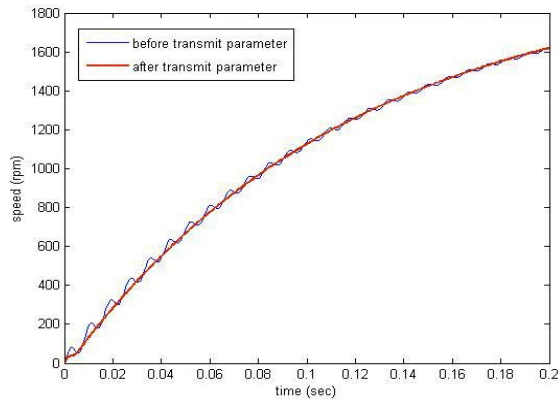


Figure 10. Normalized frequency.



(a)



(b)

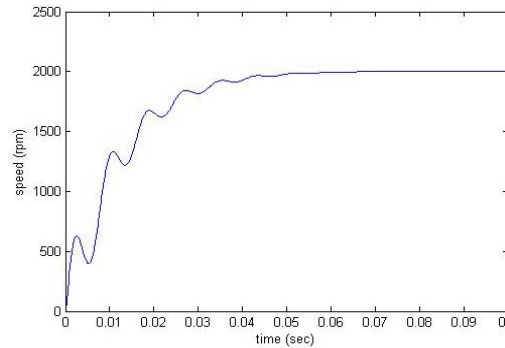
Figure 11. (a) Speed response (b) Comparison of speed response before and after parameters transmits.

calculated only, tuning parameters did not transmit into notch filter yet. At 1s, tuning part sending out parameters to notch filter to modify it. Then the transient vibration phenomenon can be repressed. The comparison of speed response before and after transmitting parameters is shown in Fig. 11(b), which is redrawn from Fig. 11(a).

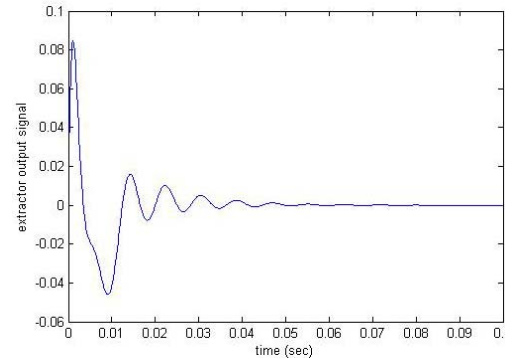
In Fig. 11(b), the blue line (vibration line) is the speed response before transmitting parameters into notch filter, the response after transmitting is the red line. It shows that the rising time in both lines are the same, and torsional vibration is suppressed clearly.

B.  $K_p = 1$

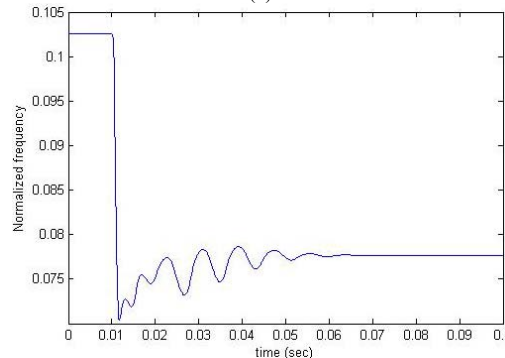
We consider now the case of large proportional gain. Fig.



(a)



(b)



(c)

Figure 12.  $K_p$  gain = 1 (a) Speed response. (b) Oscillation signal. (c) Normalized frequency.

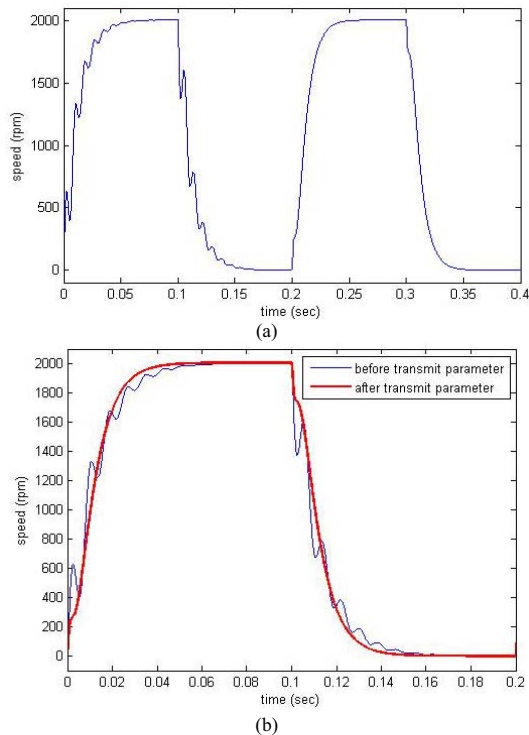


Figure 13. (a) Speed response (b) Comparison of speed response before and after parameters transmits.

12(a) is the load-motor's speed response, the oscillation signal shown in Fig. 12(b) and the Fig. 12(c) is the detected normalized frequency. In this case, the detected normalized frequency is about 0.0775, which also closed to the actual frequency.

In speed response shown in Fig. 13(a), during the 0 to 0.2s, the vibration signals are sampled calculated without transmitting parameters into notch filter. At 0.2s, tuning part sends out parameters to notch filter to modify it. Then the transient vibration phenomenon can be repressed. The comparison of speed response before and after transmitting parameters is shown in Fig. 13(b), which is redrawn from Fig. 13(a).

#### IV. CONCLUSION

There are many papers discussed the efficiency in vibration suppression of two-inertia system using adaptive notch filter. Actually some advanced servo drivers system already contained this function, but the resonance frequency repressed is in the range of several hundreds Hz or above, which is in the high frequency range, cannot using in the range around one hundred Hz or below (transient vibration type).

The design concept proposed in this paper improved the

control structure [12] which focused on high frequency repression (chattering reduction), and cannot be utilized in low frequency transient suppression. Proposed composition can be applied to low frequency repression using transient vibration signal extractor.

#### ACKNOWLEDGMENT

Research supported by NSC project 97-2221-E-009-026, NSC, Taiwan, ROC. Corresponding author E-mail: [stonecheng@mail.nctu.edu.tw](mailto:stonecheng@mail.nctu.edu.tw)

#### REFERENCES

- [1] Valenzuela, M.A., Bentley, J.M., Lorenz, R.D., "Evaluation of torsional oscillations in paper machine sections", *IEEE Trans. Ind. Appl.*, vol. 41, no. 2, pp.493-501, March/April 2005.
- [2] S.-H Song, J.-K. Ji, S.-K. sul, and M.-H. Park, "Torsional Vibration Suppression Control in 2-Mass System by State Feedback Speed Controller", *IEEE Conf., Control Appl.*, vol. 1, September 1993, pp. 129-134.
- [3] Sugiura, K. and Hori, Y., "Vibration Suppression in 2- and 3-mass System Based on the Feedback of Imperfect Derivative of the Estimated Torsional Torque", *IEEE Trans. Ind. Elec.*, vol. 43, No. 1, February 1990, pp. 56-64.
- [4] Bahr, A. and Beineke, S., "Mechanical Resonance Damping in An Industrial Servo Drive", *IEEE European Conf., Power Elec. and Appl.*, Sept. 2007, pp. 1-10.
- [5] Dhaouadi, R., Kubo, K. and Tobise, M., "Analysis and Compensation of Speed Drive Systems with Torsional Loads", *IEEE Trans. Industrial Appl.*, vol.30, No. 3, May/June 1994, pp.760-766.
- [6] Kawaharada, H., Godler, I., Ninomiya, T., Honda, H., "Vibration Suppression Control in 2-inertia System by Using Estimated Torsion Torque", *IEEE IECON*, vol. 3, Oct. 2000, pp.2219-2224.
- [7] Valenzuela, M.A.; Bentley, J.M., Villablanca, A.; Lorenz, R.D." Dynamic Compensation of Torsional Oscillation in Paper Machine Sections", *IEEE Trans. Ind. Appl.*, vol. 41, no. 6, pp.1458-1466, Nov./Dec. 2005.
- [8] Ellis, G. and Lorenz, R.D., "Resonant Load Control Methods for Industrial Servo Drives", *IEEE Conf., Industrial Appl.*, vol. 3, pp.1438-1445, Oct. 2000.
- [9] Dhaouadi R., Kubo, K. and Tobise, M., "Notch Filter Tuning for Resonant Frequency Reduction in Dual Inertia Systems", *IEEE Conf., Industrial Appl.*, Thirty-Fourth IAS Annual Meeting, vol. 3, Oct. 1999., pp.1730-173.
- [10] Huijun Wang, Dong-Hee Lee, Zhen-Guo Lee and Jin-Woo Ahn, "Vibration Rejection Scheme of Servo Drive System with Adaptive Notch Filter", *IEEE Conf, Power Elec. Spec.*, June 2006.
- [11] Tetsuaki Nagano, Aichi, "Closed-Loop Feedback Control System Having an adaptive Filter", U.S. Patent No. 5404418, Apr.4, 1995.
- [12] Tomohiro Miyazaki, "Speed Control Apparatus of Motor", U.S. Patent No. 7068923 B2, Jun.27, 2006.
- [13] Kwan, T. and Martin, K., "Adaptive Detection and Enhancement of multiple Sinusoids Using a Cascade IIR Filter", *IEEE Trans., Circ. and Syst.*, vol. 36, No. 7, July 1989.
- [14] Petraglia, M.R., Mitra, S.K. and Szczupak, J., "Adaptive sinusoid detection using IIR notch filters and multirate techniques", *IEEE Trans., Circ. and Syst. II*, vol. 41, No. 11, Nov 1994.
- [15] Petraglia, M.R., Shynk, J.J. and Mitra, S.K., "Stability bounds and steady-state coefficient variance for second-order adaptive IIR notch filter", *IEEE Trans, Signal Processing*, vol. 42, No. 7, Jul 1994.